# Model simulations of zeolite supralattices: Semiconductor Si clusters in sodalite

Alexander A. Demkov and Otto F. Sankey
*Department of Physics and Astronomy and Materials Research Center, Arizona State University, Tempe, Arizona 85287*
(Received 8 January 1997)

Periodic three-dimensional arrays of uniform nanosize clusters can be synthesized in the cages and channels of open framework materials. The aluminosilicate frameworks of zeolites have wide electronic band gaps. In addition, they are optically transparent, which opens up the possibility of forming new guest electronic states within the gap, similar to the rare-earth doping of garnets and other insulating matrices. Here we investigate theoretically the atomic geometries, energetics and electronic properties of small semiconducting Si clusters encapsulated in the all-silica sodalite $\beta$ cages. The $\beta$ cage of sodalite is a building block common to the structure of many zeolites. We find that introducing ''native'' semiconductor clusters within the cages of the host materials gives rise to extremely flat molecular electronic bands in the band gap of the host. The band gaps of the cluster can be altered by the silica potential, geometrical alteration of the cluster, and by quantum confinement. [S0163-1829(97)07740-0]

## I. INTRODUCTION

Many modern electro-optical semiconductor devices rely on spatial and quantum confinement of the electrons or holes for their operation. The best known example of this is the semiconductor superlattice,[1] which consists of artificially grown thin layers of one semiconductor material alternating on top of another. By design of layer thickness and choice of materials, electrons localize within these quasi-two-dimensional ''quantum wells.'' The electronic structure of a quantum-well device is controlled by the band structure of the bulk materials, but is modified from that by quantum confinement effects.

Nanosize clusters offer a very different mechanism of confinement. The attractive feature of clusters is that one can change their electronic properties not just incrementally (by applying magnetic and electric fields, high pressure, etc.) but drastically, by changing the constituents or structure of the cluster. Also, electronic changes in clusters are rapid, thus offering fast switching. One method to exploit the properties of small clusters is to put them in an ''inert'' supporting environment (a matrix or a host). For example, if the optical transition of a particular cluster is of practical importance, a porous glass (transparent in the spectral region of the transition) may be used as such an environment.[2] However, glasses offer little control over the cluster sizes and their interactions. Zeolite frameworks (and molecular sieves in general), on the other hand, offer a unique method for creating new three-dimensional ''supralattices'' (artificial periodic arrays of ''quantum dots'') using clusters of semiconducting (or other) materials whose dimensionality and electronic properties can be partially controlled. The large zeolite cages, from a few to several tens of angstroms across, offer lodging sites to self-assemble and stabilize clusters within the zeolite framework. These regularly spaced nanosize clusters may have the geometry of either a free cluster, a bulk fragment, or completely new structures stabilized by the encapsulation in the zeolite framework.

There has been considerable experimental effort in this area, and several new zeolite-based supralattice materials have been synthesized. The first work originated in the former Soviet Union when Bogomolov *et al.*[3] incorporated Se in zeolite X and Z. They find that Se chains self-assemble in the channels, and the optical-absorption threshold shifts upward into the blue region compared to chainlike bulk trigonal Se. This exciting observation suggested that ''quantum confinement'' produces major changes of the electron states in this system. This effect is similar to the quantum confinement that occurs in layered semiconductor superlattices, but is an order of magnitude larger.

Many subsequent experiments have incorporated clusters into the framework, and the optical-absorption threshold generally shows the ''quantum confinement'' blueshift. As specific examples we mention CdS (Ref. 4) clusters in zeolites, GaP in zeolite Y,[5] Se in mordenite,[6,7] Se in zeolites A, X, Y, AlPO-5, and mordenite,[8,9] Na clusters in sodalite,[10] PbS,[11] Pt,[12] Na-Cs alloys,[13] and K clusters in zeolite A and X.[14] This is only a partial list, and further examples can be found in review articles by Stucky and MacDougal[2] and Ozin, Kuperman, and Stein.[15] Work in this area has been partially motivated by potential applications to nonlinear optical devices and solar elements, since the $Al_{1-x}Si_xO_2$ aluminosilicate matrix has a wide band gap (transparent).

For the successful design of a supralattice the crucial question is whether the desirable properties of guest clusters will be preserved after the encapsulation, or will they be altered by the guest-guest or guest-host interactions. The guest-host interactions appear to be more important because, in a typical zeolite, guest clusters are separated by roughly ten or more angstroms, and therefore are not expected to interact strongly.

In terms of the encapsulation of the guest species by the host, the supralattices may be divided into three broad classes. The simplest class is when the guest species does not form strong covalent bonds with the host atoms of the cavity walls. The host crystal acts merely as a ''mechanical'' support for the guest species, and properties of materials of that type should be the easiest to predict. We shall call this a supralattice with *physiencapsulation* in analogy with physisorption. Examples of the physiencapsulation would be Se

 

clusters in Linde A zeolites or Se and Te chains in mordenite and cancrinite.[6,7,16–18] On the other hand, CdS clusters in zeolite Y form covalent bonds with the host atoms,[4] and we shall call this type of the encapsulation *chemiencapsulation*; its characteristic feature is a strong covalent guest-host interaction. The third class of supralattices, also with a strong guest-host interaction, we call *charge-transfer encapsulation*. In this case there is a charge transfer between the host and the guest, and ionic bonds are formed; examples of this type of encapsulation are black-sodalite, and other alkali-metal doped zeolites.[10,13,14]

The rest of this paper is organized as follows. First we briefly discuss then method, then the structural and electronic properties of silica-sodalite, and finally we discuss the electronic properties and energetics of small ''native'' Si clusters encapsulated in the cages of this structure.

## II. THEORETICAL METHODOLOGY

In this paper we examine theoretically electronic properties of supralattices by means of quantum molecular dynamics (QMD). We study the case of *physiencapsulation*, and choose as a prototype system silica-sodalite with Si clusters residing in the $\beta$ cages. To determine the equilibrium structure and the total energy of the silica-sodalite, we use the QMD method known as Fireball-96.[19] The method uses density-functional theory within the local-density approximation (LDA), and the pseudopotential approximation. The Ceperley-Alder form of the exchange-correlation potential as parameterized by Perdew and Zunger[20] is used. For silicon and oxygen, we use the ''hard'' norm-conserving pseudopotentials of the Hamann-Schlüter-Chiang[21] type. A simplified self-consistent energy functional[19] generalized from that due to Harris[22,23] is employed in a combination of the minimal basis of local ''fireball'' orbitals.[23] Forces acting on each atom are computed using a generalization of the Hellman-Feynman theorem.[23–25] The full geometrical relaxation of the internal parameters of the cubic unit cell (36 atoms for sodalite, plus up to 7 silicon guest atoms) is performed via molecular dynamics using a fictitious damping to obtain a zero force geometry. We have chosen the confinement ''fireball'' radii for the O and Si orbitals to be $r_c=3.6$ and 5.0 Bohr, respectively. Eight special $k$ points over the entire Brillouin zone are used for $k$-space intergrations, which provides convergence of the total energy to about 0.1 meV/atom.

## III. SILICA SODALITE

### A. Background

Zeolites are open framework structures that contain large polyhedral cages of atoms connected to each other by channels. The tetrahedral atom ($T$ atom) is usually Si and is surrounded by four oxygen atoms. Commonly the element Al is substituted for some of the Si atoms. In these aluminosilicates, an additional cation (e.g., Na) is incorporated interstitially within the lattice which counterbalances the charge on the Al. Smith[26] defines a zeolite as a crystalline aluminosilicate with a four-connected tetrahedral framework structure enclosing cavities occupied by large ions and water molecules, both of which have considerable freedom of movement, permitting ion exchange and reversible dehydration. However, synthetic zeolites include numerous examples that do not meet one or more of these criteria. An invaluable source of structural information on zeolites is found in Ref. 27.

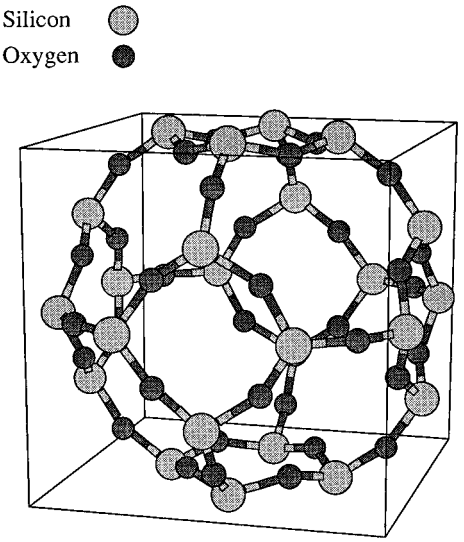


FIG. 1. The $\beta$ cage of sodalite. 24 Si atoms (lighter balls) occupy the vertices of a truncated cubo-octahedron and are connected by 36 ''bridging'' oxygen atoms (darker balls).

Synthetic zeolites play a major role in petrochemical catalysis, and also are widely used in radioactive waste storage, water treatment, gas separation and purification, and animal feed supplements. These uses are a consequence of the zeolite's exceptional ion exchange and sorption[28] properties. In addition, there is a growing interest in nontraditional applications of zeolites. These include the use of zeolites for recognition and organization of atoms, molecules, and atomic clusters. Polymers and semiconductor clusters, confined and self-assembled in zeolite pores and cages, open a new way of preparing nanoelectronic materials.[2]

The naturally occurring mineral sodalite has a unit cell composition $Na_8Al_6Si_6O_{24}Cl_2$ in which the $T$ atoms alternate between Si and Al. The structure was unraveled by Pauling in 1930.[29] Pauling suggested for sodalite a framework structure of composition $Al_6Si_6O_{24}$ made by periodically arranging Kelvin's polyhedra (also called $\beta$ cages) in a simple cubic lattice. Kelvin's polyhedron[30] is a truncated octahedron familiar among solid-state physicists, since geometrically it is the first Brillouin zone of the bcc reciprocal lattice (fcc direct lattice). This structure was confirmed by the later experiments of Löns and Schulz.[31]

Silica sodalite is the all-silicon ($SiO_2$) version of the zeolite sodalite. The unit-cell composition is $Si_{12}O_{24}$, and all tetrahedral atoms ($T$ atoms) are Si. Figure 1 shows the $\beta$ cage of silica sodalite $Si_{12}O_{24}$. The framework is constructed of corner-sharing tetrahedra ($SiO_4$) with ''rooms and passages'' that can be occupied by guest molecules. In 1985 Bibby and Dale reported the nonaqueous synthesis of a novel pure-silica form of sodalite.[32] The unit cell dimension was determined from the x-ray powder diffraction pattern to be 8.836 Å. They pointed out that unlike the rest of low-density pure silica polymorphs, silica sodalite contains only six- and

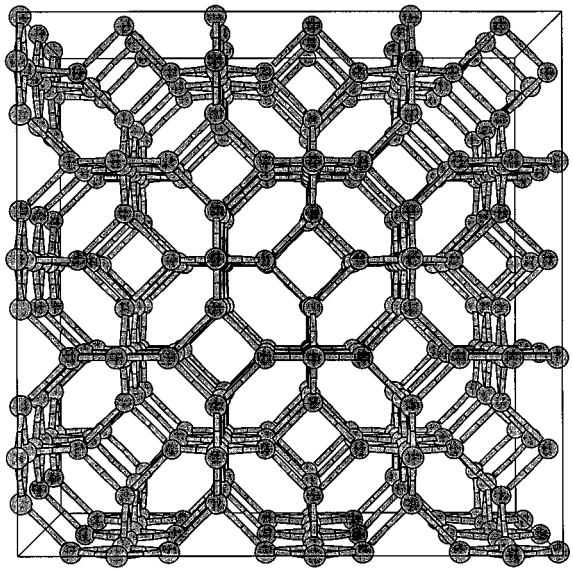

FIG. 2. The structure of the simple cubic sodalite lattice. Only the $T$ atoms (Si) are shown. Each cage consists of a truncated cubo-octahedron of 24 atoms of eight hexagons and six squares.

four-membered rings. Richardson *et al.*[33] in a later paper reported a refined structure. The space group for silica sodalite is $Im3m$. Silicon atoms are at sites $12d$, and framework oxygen atoms are at sites $24h$. The structure of silica sodalite is shown in Fig. 2. The lattice is simple cubic obtained by stacking truncated cubooctahedra ($\beta$ cages) to fill all space. There are 12 $T$ atoms/cell and 24 oxygen bridging atoms (not shown in Fig. 2) connecting the vertices. Each unit cell contains two such cages, but each atom is shared between four cages.

There have been several theoretical studies of silica sodalite reported. Vibrational properties have been studied both by the lattice dynamics method[34,35] and by molecular dynamics.[36] Teter *et al.*[37] have recently performed *ab initio* calculations of several silica polymorphs to determine their cohesive energies including Al-free sodalite, and their results are in reasonable agreement with experiment.[33]

### B. Results

Using the quantum molecular-dynamics method here, we find an equilibrium cubic lattice constant of 8.6 Å (expt. $\sim$8.84 Å), and the equilibrium Si-O distances $d_{\text{Si-O}}$ to be in the range from 1.545 to 1.547 Å (experiments $\sim$1.59 Å), the tetrahedral-like O-$T$-O angle to be 109.14°–110.12°, and the $T$-O-$T$ angle $\theta$ to be 158.48°–159.34° (experiment $\sim$159.7°). The Löwdin charges are $-0.6286$, and $+1.2572$, for oxygen and silicon, respectively. Our method consistently underestimates the bond lengths of silica by about 2.7%.[19] This discrepancy between the calculations and the experiment may be attributed first to the usual overbinding of the LDA. More importantly, the discrepancy may be due to the particular approximations we use in our technique, such as the representation of the electron density, linearization of the exchange-correlation potential, and the use of local orbitals.[23,19] In addition, our calculations neglect temperature effects, while experiments are usually done at room temperature. However, we find the significant result that silica sodalite is just $0.12\ \text{eV/SiO}_2$ higher in total energy than $\alpha$-quartz.[19] This finding is in qualitative agreement with the recent thermochemical study of Petrovic *et al.*,[38] who find that silica structures of large volume are typically $0.10-0.14\ \text{eV/SiO}_2$ above $\alpha$-quartz, although there are no data to our knowledge specifically for silica sodalite.

The fairly low energy of silica sodalite with respect to $\alpha$-quartz may be understood in terms of a simple model, previously suggested for the energetics of silica cristobalite.[19] The model is based on the intricate connection between Si-O bond length and Si-O-Si bond angle. The effect of bond-angle/bond-length correlations on the energetics of silica polymorphs is obtained generalizing the following expression obtained from $\beta$-cristobalite,

$$E(d,\phi)=E_0+\frac{1}{2}k(d-d_b)^2+\frac{1}{2}\kappa_0\left(1-\frac{d}{d^*}\right)\phi^2+\frac{1}{4!}\kappa_4\phi^4. \tag{1}$$

Here $E(d,\phi)$ is energy as a function of two independent variables—the Si-O bond length $d$, and the rotation angle $\phi$ between rigid tetrahedra[39] [this angle is related to the $T$-O-$T$ angle $\Theta$ as $\cos\Theta=(1-4\cos^2\phi)/3$]. Typically the angle $\Theta$ is about 150°, but wide angles ($\Theta=180°$ corresponding to $\phi=0°$) are not uncommon in zeolites. However, small angles (the limit being $\Theta=109°$ or $\phi=45°$) are rare. The parameters $\kappa_0$, $k$, $d$, and $d^*$ have been determined for $\beta$-cristobalite, and are in Table III of Ref. 19. Thus the expansion in Eq. (1) is performed around the wide-angle linear Si-O-Si system ($\phi=0$) where the minimum-energy Si-O bond length $d_{\text{Si-O}}$ is defined to be the value $d_b$. The zero pressure minimum-energy structure is found by imposing $\partial E/\partial d=\partial E/\partial\phi=0$. The vanishing of $\partial E/\partial d$ leads to

$$d_{\min}=d_b+(\kappa_0/2d^*k)\,\phi_{\min}^2. \tag{2}$$

Equation (2) gives a *single closed* form relation between bond length and Si-O-Si bond angle. The relation shows that systems with a larger Si-O-Si bond angle (i.e., more linear Si-O-Si bond with smaller tilt angle $\phi_{\min}$) have a shorter bond length, and vice versa. We use the parameters $\kappa_0$, $k$, $d$, and $d^*$ from Ref. 19 here, and relate the changes of bond length to changes of angle using Eq. (2) with the result

$$-\frac{\delta\Theta}{\Theta_{\beta c}}=9.9\,\frac{\delta d}{d_{\beta c}}. \tag{3}$$

In this equation we use the angle $\Theta_{\beta c}$ and the bond length $d_{\beta c}$ of $\beta$-cristobalite as a ''standard,'' and Eq. (3) then predicts a change in bond angle in any other material, $\delta\Theta=\Theta-\Theta_{\beta c}$, versus the change in bond length, $\delta d=d-d_{\beta c}$, of that material.

We now apply this to silica sodalite. First we notice how small changes in bond length become ''magnified'' by nearly a factor of 10 to produce changes in bond angle—e.g., a 1% change in bond length produces a 9.9% change in Si-O-Si bond angle. The average Si-O bond length in silica sodalite ($d=1.55$ Å) is calculated to be about 1% shorter than that in $\beta$-cristobalite (1.56 Å). For the energy of the sodalite structure to be low with this reduced bond length, the $T$-O-$T$ angle must ''open up.'' This is indeed very close

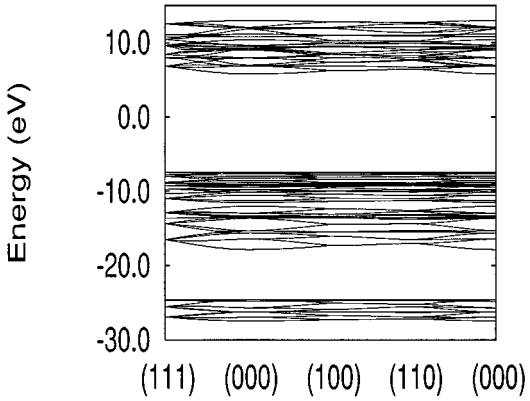


FIG. 3. The electronic band structure of pure silica sodalite ($Si_{12}O_{24}$). The valence-band maximum is near $-7$ eV and the conduction band minimum is near $+7$ eV.

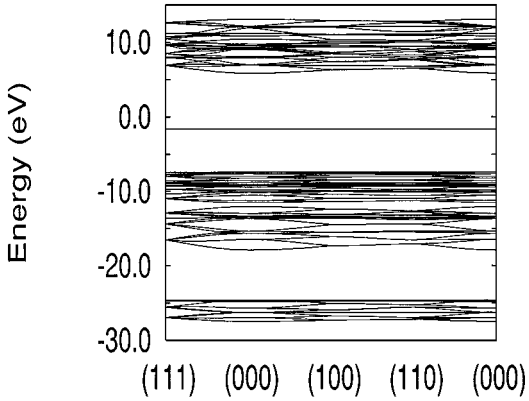


FIG. 4. The band structure of the simplest supralattice: Si encapsulated in every other $\beta$ cage of silica sodalite ($Si_1@Si_{12}O_{24}$). The state near $-2.0$ eV is a triply degenerate $p$ level of $Si_1$.

to what we find for the bond angle from the QMD simulation. In sodalite the electronic structure model gives $\Theta = 159°$, while in $\beta$-cristobalite we find $\Theta = 147°$. There is an almost 8% increase in the $T$-O-$T$ angle in sodalite compared to that of $\beta$-cristobalite, which is very close to the 9.9% predicted by the analytical model. Experimentally, the Si-O bond length and the Si-O-Si angle in $\beta$-cristobalite are 1.6 Å and 147.8°, respectively, while in silica sodalite they are 1.59 Å and 159.7°.

The electronic band structure of silica sodalite is shown in Fig. 3. Overall, the basic features are similar to that of other silicas.[19] There are oxygen $s$ state derived bands in the range $-28$ eV to $-25$ eV. The next highest set of bands are the oxygen-silicon bonding orbital bands centered at around $-16$ to $-12$ eV. The next highest set of occupied bands around $-12$ to $-8$ eV is dominated by the nonbonding $p_\pi$ states of oxygen. These states form the top of the occupied valence band. The bottom of the unoccupied conduction band at $\sim +7.0$ eV and is singly degenerate. The band gap between the top of the valence band and the conduction band is direct ($\Gamma$-to-$\Gamma$) and is 14 eV. This bandgap is too large compared to experiment, although LDA typically predicts gaps below those of experiment. However, the use of a minimal basis set of local orbitals (the main effect here) tends to increase[40] the band gap above experiment. When compared to an identical calculation on $\alpha$-quartz[19] the sodalite band gap is about 2 eV smaller.

Concluding this section, we have investigated the energetics, atomic structure, and the band structure of silica sodalite. We find the cubic lattice constant to be 8.6 Å or 2.7% smaller than experiment. The relaxed structure reproduces the expected trend in the bond-length/bond-angle correlation predicted by a simple analytical model.[19] The material is found to be a wide-band-gap insulator.

## IV. SI CLUSTERS IN SILICA SODALITE

In this section, we investigate the electronic properties of a model supralattice with the physiencapsulation of semiconducting clusters.[41] To explore the possibility of creating new structures and materials we study the simpliest ''model'' system—''native'' Si clusters in silica sodalite. The choice of system is based on the fact that both silicon clusters and silica sodalite represent the simplest choice for both the cluster and the zeolite system. In addition, the $\beta$ cage of sodalite is a structural element common to many zeolites. We have studied clusters from one to seven Si atoms in the $\beta$ cage, but discuss in detail in the first subsection the electronic structures only of the smallest ($Si_1$) and largest ($Si_5$) clusters that one might expect to fit inside the sodalite cages. In the final subsection, we describe the energetics of simple silicon clusters inside the cages, and their energy landscape.

### A. Electronic properties

We now investigate the electronic properties of Si clusters in the sodalite cage. We begin by considering a single Si atom in the center of one of the two cages in the unit cell. These interstitial centers are of high $O_h$ symmetry. The geometry of the host crystal was held fixed. The caged Si atoms are 8.6 Å apart, that is, they are separated by the lattice constant. The resulting electronic band structure is shown in Fig. 4. The most noticable effect of the interstitial Si atom on the band structure is the appearance of a triply degenerate ($p$-like) level very near the middle of the band gap (at $\sim -2.0$ eV). This triply degenerate band (occupied with the two electrons) retains the character of the atomic $p$ state of silicon, and shows almost no dispersion with wave vector. This system then, according to single electron theory, is metallic. However, since the width of the band is less than $kT$ at room temperature, correlation effects will dominate and the material is likely a Mott insulator. An additional $s$ state of Si is also incorporated into the band structure near $\sim -9.2$ eV, but it is resonant with the crystal states of the host and cannot be easily seen in the figure. Generally, apart from these atomiclike Si states, the band structure the composite material is quite similar to pristine silica sodalite of Fig. 3.

This calculation shows there is very little interaction between a single guest Si atom and the host. This can be understood in the following way. When a Si atom is introduced in the middle of the $\beta$ cage there are no close neighbors. The first nearest neighbors are the oxygen atoms of the cage which are at a distance of $\sim 3$ Å (compared with the $d_{\text{Si-O}}$ distance of a 1.6 Å in the silica), and the second nearest neighbors are silicon atoms about 4.0 Å distant. The first neighbors in diamond Si are at 2.35 Å. Therefore, the hop-

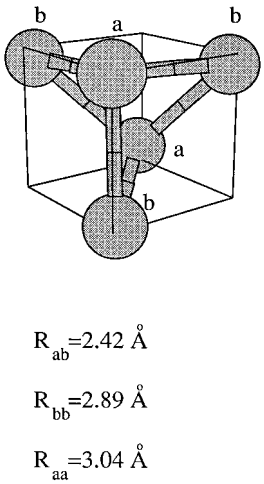


FIG. 5. The lowest-energy geometry of a $Si_5$ cluster inside the zeolite found by the QMD simulation. The structure is a trigonal bipyramid, consisting of the equilateral triangle with one atom above the triangle and one atom below. In the figure, the *b* atoms are in the basal plane of the triangle and apex *a* atoms are out of the plane.

ping from the caged Si atom to the surrounding host ''cage'' states is very small. Since the *p*-level of the caged silicon atom is ''out of resonance'' with the silica states, and the hopping integral is small, the state retains its atomic character.

We now consider a $Si_5$ cluster inside the $\beta$ cage. Again only one cage of the two within the unit cell is occupied. The lowest-energy geometry of a $Si_5$ cluster inside the zeolite found by the QMD simulation is shown in Fig. 5. This geometry is surprisingly similar to that calculated for a $Si_5$ cluster in free space.[43] The structure is a trigonal bipyramid, consisting of an equilateral triangle (*b* atoms of Fig. 5) with one atom above the triangle and one atom below (*a* atoms). We find $R_{aa}=3.04$ Å, $R_{bb}=2.89$ Å, and $R_{ab}=2.42$ Å, which should be compared with 2.98 Å, 3.0 Å, and 2.29 Å, respectively, found using the current technique for a free cluster (in good agreement with previously published results[43–45] for the free cluster). The encapsulated cluster, is overall, neutral. However, the *a* atoms are slightly positive $(+0.03e)$, while the *b* atoms are slightly negative $(-0.02e)$. The volume of the bipyramid corresponding to a free cluster is 4.86 $Å^3$, while that of the cluster inside the zeolite cage is 4.76 $Å^3$, which is a 2% volume reduction. If we compare the total energies calculated for the two geometries (one of that of the free cluster geometry and of that of the constrained cluster) there is the energy increase of 0.042 eV/cluster upon compression. This can be loosely interpreted as 67 GPa pressure $(-\Delta E/\Delta V)$ excerted on the cluster by the zeolite. An interesting consequence of such an effect would be the change of the melting temperature of the guest material, as likely seen with Se clusters in zeolite Y.[9]

The band structure of the supralattice of $Si_5$ clusters encapsulated inside the $\beta$ cages of sodalite is shown in Fig. 6. Even for this large cluster, the electronic states of the guest cluster appear in the gap region of sodalite, and are very similar to those of the free cluster. There is, however, an upward shift in energy due to the potential from long-range

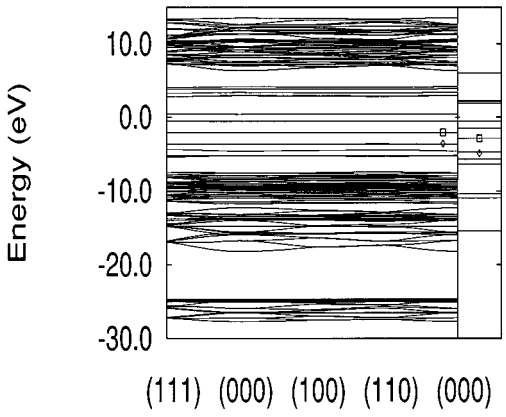


FIG. 6. The band structure of the supralattice: $Si_5$ clusters encapsulated in every other $\beta$ cage of silica sodalite. On the right of the figure are the molecular orbitals of a free $Si_5$ cluster with the same geometry as in the sodalite host. The diamond and square indicate the HOMO and LUMO, respectively.

Coulomb effects of the silica (see below). There are no unoccupied states of the cluster under the valence-band edge of the host, and there is negligible charge transfer between sodalite and the cluster. The highest occupied molecular orbital (HOMO) of the encapsulated cluster is at $-3.64$ eV, and the lowest occupied molecular orbital (LUMO) is at $-2.09$ eV, which gives a gap of 1.55 eV. The HOMO is doubly degenerate, and the LUMO in nondegenerate. The HOMO-LUMO gap of the $Si_5$ cluster in free space, calculated for comparison, is found to be 2.07 eV. This system then shows the opposite effect of a simple quantum confinement model. To investigate the origin of this band-gap reduction we calculate the electronic states of a free cluster, but with the compressed geometry found for the cluster inside the sodalite cage (see Fig. 5). We find that the HOMO does not change upon compression, while the nondegenerate LUMO state moves down in energy by 0.33 eV. Thus an important reduction of the HOMO-LUMO gap is produced by the change in the geometry of the cluster (a ''pressure'' effect). In addition to this effect, the states of the cluster are influenced by the sodalite potential. When the cluster is put inside the cage, it ''feels'' the nonuniform potential due to the silica, even though there is little bonding interaction with the atoms of the host. It is because of this nonuniformity of the potential that states with different spacial character are affected differently. The HOMO is shifted up by 1.3 eV, while the LUMO is shifted up by only 1.1 eV, which results in an additional closure of the gap. We emphasize that the effect of the sodalite potential is comparable in magnitude with the pressure effect. In this particular example, both effects cause the energy gap to close, but it is not inconceivable that in other clusters the two effects partially cancel each other. Therefore, any simplified picture predicting the electronic properties of a supralattice should be considered with a great deal of caution.

We illustrate the results for $Si_5$ in Fig. 7; (a) shows the HOMO and LUMO of the unconstrained (fully geometrically relaxed) $Si_5$ cluster in free space, (b) shows the pressure effect (the cluster in free space in the geometry constrained to that forced by the encapsulation), and (c) shows the combined (a geometrical constraint plus the nonuniform potential

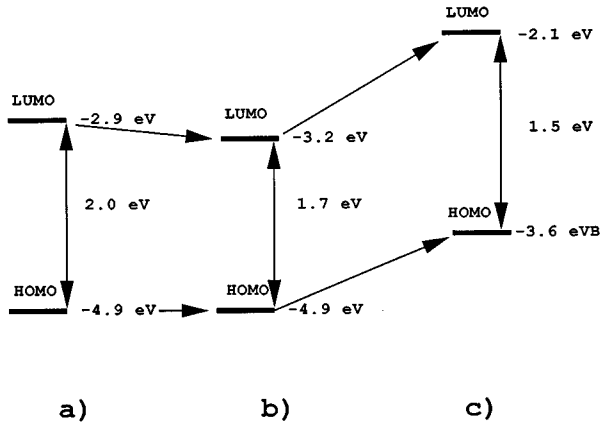


FIG. 7. (a) Schematic energy-level diagram for $Si_5$ cluster; (a) shows the HOMO and LUMO of the unconstrained (fully geometrically relaxed) $Si_5$ cluster in free space, (b) shows the pressure effect—the cluster in free space in the geometry constrained to that forced by the encapsulation, and (c) shows the total effect of the encapsulation. The overall reduction of the HOMO-LUMO splitting in (c) is due to a combination of both the pressure (a geometrical constraint) and ''electrostatic'' (the nonuniform potential inside the cage) effects.

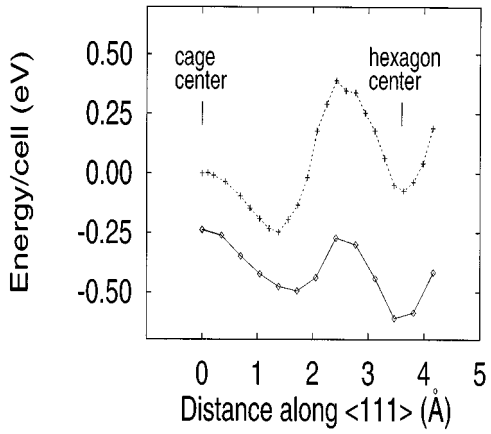


FIG. 8. The potential-energy profile along the (111) direction for a single Si atom encapsulated in every other $\beta$ cage of silica sodalite. The solid line is the result of the dynamic calculation and the dashed line is the result of the static calculation (see text). The initial distortion away from the origin is due to a Jahn-Teller effect.

inside the cage) effect of the encapsulation. Our technique, as it has been mentioned, tends to overestimate band gaps; for bulk Si we calculate the band gap of 1.86 eV (expt. 1.1–1.2 eV). Therefore, the new composite material ($Si_5@Si_6O_{12}$) is expected to have a band gap only slightly smaller than that of bulk diamond phase silicon, but with almost no dispersion of the band edges.

For these native clusters, we find that the electronic structure of Si guest clusters is somewhat altered by the cluster-host interaction. But the origin of the states in the energy gap region of the host matrix can be easily traced to the states of the cluster. This is in contrast to the case of alkali metal atoms in sodalite where the electronic states of the cluster inside the zeolite are perhaps better described as ''cavity states'' and are controlled by the zeolite.[46,47] This suggests that one perhaps can form a new material with the electronic gap reminiscent of that of the cluster—e.g., silica sodalite ''doped'' with $Si_5$ is a direct-band-gap material with a band gap slightly below that of bulk silicon; however, the details of the band structure are difficult to control.

### B. Energetics of Si clusters

We now discuss the energetics of Si clusters inside the silica-sodalite cages. We first consider a single Si atom residing in the middle of the sodalite cage. The fact that the highest occupied states are partially occupied and triply degenerate suggests a Jahn-Teller instability. This is indeed the case. In Fig. 8 we show the ''dynamic'' energy profile (solid line) experienced by a single Si atom when moved in the (111) direction along the line connecting the centers of the two adjacent cages. Such a line would pass through the center of the hexagonal faces of the $\beta$ cages. The dynamic calculation of the energy is done in the following way—the guest atom is assigned an infinitely large mass, so it cannot move during the molecular-dynamics relaxation. The position of the guest atom is changed discretely along the (111) direction and at each fixed position the host system is allowed to relax to the minimum-energy configuration. From Fig. 8 it is clear that the guest Si atom prefers to move away from the center of the $\beta$ cage (approximately 1.75 Å off center). Also, we find that the 6 ring [located about 3.7 Å away from the center of the cage in the (111) direction] acts like a trap for the impurity atom. Both phenomena are well known for cation metals in zeolite structures. The relaxation of the framework is found to be important in determining the preferred equilibrium site of the guest atom. This is illustrated by a static calculation shown in Fig. 8 (dashed line) in which the guest atom is moved discretely, but the $SiO_2$ framework is not allowed to relax towards its equilibrium configuration. Note, that even though both methods (static and dynamic) produce two local minima at nearly the same coordinate of the guest, the absolute minima for the two methods are different. Framework relaxation is often neglected in guest-host systems,[42] and our results show that even for this particularly simple system it is important.

We have studied the structure and energetics of the clusters $Si_2$, $Si_3$, $Si_4$, $Si_5$, $Si_6$, and $Si_7$. Full geometrical optimization of the clusters and the framework was performed. The structure of the Si clusters inside the cages of silica sodalite in general closely resembles that of the clusters in free space. For the dimer we find two configurations, a metastable ''short dimer'' with Si-Si bond length of 2.03 Å, and a ''long dimer'' with Si-Si bond length of 2.28 Å, similar to the results of Sankey *et al.*[43] for clusters in free space. For $Si_3$ we find the ground-state configuration to be an isosceles triangle with two shorter Si-Si bonds of 2.17 Å at a 74.52° angle and the apex atom slightly overcharged ($-0.06e$). These bond lengths and angle are slightly smaller than those found for a ''free'' trimer; 2.19 Å and 76.25°, respectively. Furthermore, for $Si_4$ we find the tetrahedron, and not the rhombus, to be the ground state. This may be an example of a more general phenomenon—the cluster inside a zeolite cage adopts a more compact geometry when it is big enough to feel the pressure of the walls of the cavity. $Si_5$ and $Si_6$ both form biprisms that are about 6% smaller along the highest-order symmetry axis than their ''free space'' analogs, which

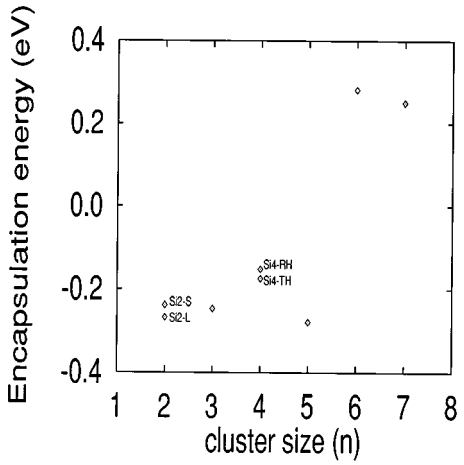


FIG. 9. The energy of encapsulation for Si clusters in silica sodalite. For the $Si_2$ and $Si_4$ clusters, energies for two different configurations are shown. Si2-*S* and Si2-*L* stand for the short and long dimers, respectively; Si4-*RH* and Si4-*TH* stand for the rhombus and tetrahedron. Negative energies mean that a cluster has lower energy inside a silica sodalite cage than in free space.

is compensated by a 2% increase in the Si-Si bond length. $Si_7$ is found to be unstable towards the decomposition into $Si_6$ and a single Si atom trapped in the vicinity of the 4 ring of the sodalite cage.

When we look into energetics of encapsulation of these clusters we find that only the $Si_n$ clusters with $n \leqslant 5$ have negative energies of encapsulation. The energy of encapsulation $E_{\rm enc}$ is defined in the following way: $nE_{\rm enc} = E(\mathrm{Si}_n + \mathrm{sodalite}) - E(\mathrm{Si}_n) - E(\mathrm{sodalite})$, and measures the cost of cluster encapsulation per Si atom inside sodalite. Here $E(\mathrm{Si}_n)$ is the energy of a free space cluster of $Si_n$. The energy of encapsulation is shown in Fig. 9. Energies for two different configurations of the $Si_2$ and $Si_4$ clusters are shown, Si2-*S* and Si2-*L* stand for the short and long dimers, respectively; Si4-*RH* and Si4-*TH* stand for the rhombus and tetrahedron. The transition from negative to positive energy may be understood using the following argument. The volume of the $\beta$ cage is approximately 113 $\text{Å}^3$ (assuming it is a sphere with the ''effective'' radius of 3 Å), while the volume per atom in the diamond phase of Si is 20.2 $\text{Å}^3$. Hence a Si cluster is ''squeezed'' when $Si_6$ or $Si_7$ is put inside the cage.

## V. CONCLUSIONS

We have investigated loading of zeolite cages with small semiconductor clusters. Nanocomposites of this type are known as supralattices, and offer a unique way to exploit the electronic properties of small clusters in designing advanced electronic materials. As a ''model'' system we have studied small ''native'' Si clusters in silica sodalite. We use QMD, which enables us to perform the structural optimization of the system and to investigate its electronic properties within a unified theoretical framework. Modeling electronic materials with clusters encapsulated in zeolites opens up a new avenue in band-gap engineering and materials design. Our results show that when supralattices are studied for electronic applications, it is of principal importance to address both the geometry and the electronic spectrum simultaniously. We find that sufficiently small Si clusters exhibit very little interaction with the host and form a ''molecular crystal''-like arrangement with the periodicity dictated by the host. However, one should not neglect the structural relaxation of the host crystalline matrix in response to the presense of the guest cluster.

We have investigated silica sodalite. We find the cubic lattice constant to be 8.6 Å or 3% smaller than the experimental one. The relaxed structure reproduces the general trend in the bond-length/bond-angle correlation well described by a simple analytical model.[19] The material is found to be a wide-band-gap insulator with the band gap about 2 eV smaller than that of $\alpha$-quartz. We find silica sodalite to have a cohesive energy of about 0.12 $\text{eV}/\text{SiO}_2$ (12 kJ/mol) above $\alpha$-quartz, in a good agreement with the recent thermochemical trends[38] where it is found that structures of expanded volume are typically 0.10–14 kJ/mole above $\alpha$-quartz.

We have studied the structure, electronic properties, and energetics of the native clusters $Si_2$, $Si_3$, $Si_4$, $Si_5$, $Si_6$, and $Si_7$ in silica sodalite. The geometrical structure of sufficiently small clusters ($Si_n$ clusters with $n \leqslant 5$) is similar to that of clusters in free space. There are some differences, such as the fact that $Si_4$ prefers a more dense tetrahedral structure when it is inside the sodalite $\beta$ cage, rather than the rhombohedral form found for this cluster in free space. This result is in agreement with the notion that inside zeolite cages semiconductor clusters find geometries reminiscent of high-pressure phases rather than the ground-state bulk materials, as has been observed experimentally for CdS in zeolite Y.[4]

Electronically, the doping results in the formation of the molecular electronic states in the band-gap region of the host. A strong guest-host interaction is expected only when the electronic states of the guest are in ''resonance'' with the band states of the host as in the case of e.g., Zn and S in $SiO_2$, or for the alkali-metal doping. We find that the electronic structure of Si clusters is altered by the cluster-host interaction, but the electronic states responsible for the optical properties of the nanocomposite supralattice retain their cluster character. These states are affected via two different mechanisms. Both the change in the geometry of the cluster caused by encapsulation (pressurelike effect), and the electric potential inside the cages of the host (''electrostatic'' effect) cause the shifts of the cluster states. This suggests that one can form a new material with the electronic gap stemming from that of the cluster—e.g., silica sodalite ''doped'' with $Si_5$ is a direct-band-gap material with a band gap slightly smaller than that of bulk silicon. However, each cluster has different electronic properties and in practice it may be difficult to achieve precise control of the energy gap magnitude.

## ACKNOWLEDGMENTS

We thank the NSF (Grant No. DMR-95-26274) for support. It is our pleasure to thank Dr. Nick Blake for many insightful discussions that we had in the course of this work.

[1] L. Esaki and R. Tsu, J. Rev. Dev. **14**, 61 (1970).
[2] J. E. Mac Dougall and G. D. Stuckey, in *On Clusters and Clustering, From Atoms to Fractals*, edited by P. J. Reynolds (Elsevier Science, New York, 1993), p. 273; G. D. Stucky and J. E. Mac Dougall, Science **247**, 669 (1990).
[3] V. N. Bogomolov, E. L. Lutsenko, V. P. Petranovskii, and S. V. Kholodkevich, Pis'ma Zh. Eksp. Teor. Fiz. **23** 528 (1976) [JETP Lett. **23**, 483 (1976)]; V. N. Bogomolov, S. V. Kholodkevich, S. G. Romanov, and L. S. Agroskin, Solid State Commun. **47**, 181 (1983).
[4] Y. Wang and N. Herron, J. Phys. Chem. **92**, 4988 (1988).
[5] J. E. MacDougall, H. Eckert, G. D. Stucky, N. Herron, Y. Wang, K. Moller, T. Bein, and D. Cox, J. Am. Chem. Soc. **111**, 8006 (1989).
[6] K. Tamura, S. Hosokawa, H. Endo, S. Yamasaki, and H. Oyanagi, J. Phys. Soc. Jpn. **55**, 528 (1986).
[7] Y. Katayama, M. Yao, Y. Ajiro, M. Inui, and H. Endo, J. Phys. Soc. Jpn. **58**, 1811 (1989).
[8] J. B. Parise, J. E. MacDougall, N. Herron, R. Farlee, A. W. Sleight, Y. Wang, T. Bein, K. Moller, and L. M. Moroney, Inorg. Chem. **27**, 221 (1988).
[9] A. Goldbach, L. Iton, M. Grimsditch, and M.-L. Saboungi, J. Am. Chem. Soc. **118**, 2004 (1996).
[10] J. B. Smeulders, M. A. Hefni, A. A. K. Klaassen, E. de Boer, U. Westphal, and G. Geismar, Zeolites **7**, 347 (1987).
[11] K. Moller, T. Bein, N. Herron, W. Mahler, and Y. Wang, Inorg. Chem. **28**, 2914 (1989).
[12] M. G. Samant and M. Boudart, J. Phys. Chem. **95**, 4070 (1991).
[13] F. Blatter, R. W. Blazey, and A. M. Portis, Phys. Rev. B **44**, 2800 (1991).
[14] T. Sun and K. Seff, J. Phys. Chem. **97**, 5213 (1993).
[15] G. A. Ozin, A. Kuperman, and A. Stein, Angew. Chem. Int. Ed. Engl. **28**, 359 (1989).
[16] Y. Nozue, T. Kodaira, O. Terasaki, Y. Yamazaki, T. Goto, D. Watanabe, and J. M. Thomas, J. Phys.: Condens. Matter **2**, 5209 (1990).
[17] L. Khouchaf, M.-H. Tuilier, J. L. Guth, and B. Elouadi, J. Phys. Chem. Solids **57**, 251 (1996).
[18] V. V. Poborchii, J. Phys. Chem. Solids **55**, 737 (1994).
[19] A. A. Demkov, J. Ortega, O. F. Sankey, and M. P. Grumbach, Phys. Rev. B **52**, 1618 (1995).
[20] D. M. Ceperley and B. J. Alder, Phys. Rev. Lett. **45**, 566 (1980); J. Perdew and A. Zunger, Phys. Rev. B **23**, 5048 (1981).
[21] D. R. Hamann, M. Schlüter, and C. Chiang, Phys. Rev. Lett. **43**, 1494 (1979).
[22] J. Harris, Phys. Rev. B **31**, 1770 (1985).
[23] O. F. Sankey and D. J. Niklewski, Phys. Rev. B **40**, 3979 (1989).
[24] H. Hellmann, *Einfuhrung in die Quantumchemie* (Franz Deutsche, Leipzig, 1937).
[25] R. P. Feynman, Phys. Rev. **56**, 340 (1939).
[26] J. V. Smith, Chem. Rev. **88**, 149 (1988).
[27] W. M. Meier and D. H. Olson, *Atlas of Zeolite Structure Types*, 3rd ed. (Butterworth-Heineman, London, 1992).
[28] A. Dyer, Chem. Ind. 241 (1984).
[29] L. Pauling, Z. Kristallogr. **74**, 213 (1930).
[30] W. Thomson, Lond. Edinb. Dublin Philos. Mag. J. Sci. **24**, 503 (1887).
[31] V. J. Löns and H. Schulz, Acta Crystallogr. **23**, 434 (1967).
[32] D. M. Bibby and M. P. Dale, Nature (London) **317**, 157 (1985).
[33] J. W. Richardson, J. J. Pluth, J. V. Smith, W. J. Dytrich, and D. M. Bibby, J. Phys. Chem. **92**, 243 (1988).
[34] J. B. Nicholas, A. J. Hopfinger, F. R. Trouw, and L. E. Iton, J. Am. Chem. Soc. **113**, 4792 (1991).
[35] A. J. M. De Man, B. W. H. van Beest, M. Leslie, and R. A. van Santen, J. Phys. Chem. **94**, 2524 (1990).
[36] K. S. Smirnov and D. Bougeard, J. Phys. Chem. **97**, 9434 (1993).
[37] D. M. Teter, G. V. Gibbs, M. B. Boisen, Jr., M. P. Teter, and D. C. Allan, Phys. Rev. B **52**, 8064 (1995).
[38] I. Petrovic, A. Navrotsky, M. Davis, and S. I. Zones, Chem. Mater. **5**, 1805 (1993).
[39] M. O'Keeffe and B. Hyde, Acta Crystallogr. Sect. B **32**, 2923 (1977).
[40] R. W. Jansen and O. F. Sankey, Phys. Rev. B **36**, 6520 (1987).
[41] A. A. Demkov and O. F. Sankey, J. Comput. Aided. Mater. Des. **3**, 128 (1996).
[42] C. P. Ursenbach, P. A. Madden, I. Stich, and M. C. Payne, J. Phys. Chem. **99**, 6697 (1995).
[43] O. F. Sankey, D. J. Niklewski, D. A. Drabold, and J. D. Dow, Phys. Rev. B **41**, 12 750 (1990).
[44] K Ragavachari and V. Logovinsky, Phys. Rev. Lett. **55**, 2853 (1986).
[45] D. Tomanek and M. A. Schlüter, Phys. Rev. B **36**, 1208 (1987).
[46] N. P. Blake, V. I. Srdanov, and H. Matiu, J. Phys. Chem. **99**, 2127 (1995).
[47] O. F. Sankey and A. A. Demkov (unpublished).